Blade Pressure Data
NASA/US Army Benchmark Hover Test

Norman W. Schaeffler
Flow Physics and Control Branch
NASA Langley Research Center

Release 1: October, 2023

1 Overview of the Blades and Blade Pressures

An overview of the Benchmark Hover Test is provided in Norman et al. [1] and the text provided here is to provide context for the blade pressure data acquired during the test and is largely based on the presentation in Norman et al.

The Hover Validation and Acoustic Baseline (HVAB) blade set was a new pressure-instrumented rotor developed and fabricated specifically for the Benchmark Hover Test. The HVAB blade set was designed as a four-bladed, articulated rotor with pressure and structural instrumentation. The rotor incorporates publicly available RC series airfoils and is geometrically identical (except for the blade root) to the Army PSP rotor that was previously tested at Langley Research Center [2, 3].

A detailed description of the entire six-bladed HVAB rotor blade set, including the as-designed geometry, instrumentation, and structural properties, is provided in a NASA TM [4]. Of particular concern here is the first pressure-instrumented blade, the Hover blade (SN004). This blade was designed to incorporate 187 unsteady absolute pressure transducers, arranged in 11 chordwise stations consisting of 17 transducers each.

One of the key rotor design requirements for the HVAB blade set was for blade uniformity despite the differences in instrumentation between blades. For each of the blades without pressure transducers, representative masses for the transducers and wiring were installed in the same transducer locations that were defined for SN004. This resulted in a set of blades with essentially the same mass distribution down the lengths of the blades. Each blade was also balanced against the Hover blade, SN004, ensuring that the calculated centrifugal forces at the maximum operational RPM of 1310 were within $\pm 5\ lbf$ of the mean value for all the blades. Additionally, for the blades tested in this research effort, the measured natural frequencies for the first six modes were within $\pm 5\%$ of the average values across the set of blades.

2 Blade Pressures and Rotating Data Acquisition System

The 187 unsteady absolute pressure transducers in the Hover blade were arranged in 11 chordwise stations of 17 transducers each. For each station, six of the transducers were located on the lower surface and 11 were located on the upper surface, with the first upper surface transducer being located near the leading edge of the blade. The blade stations were numbered in sequence starting at Station 1, which is closest to the root of the blade at 0.397R, and proceeding to Station 11, which is closest to the tip at 0.988R.

During testing, the voltages from the pressure transducers were acquired exclusively in the rotating frame by the hub-mounted Rotating Data Acquisition System (RDAS). All 256 data channels on the RDAS are

acquired simultaneously and each channel has its own programmable amplification and conditioning circuitry and analog-to-digital convertor. The sampling rate for all channels was 48,800 samples per second. To align the RDAS data and the facility data, there were four timing signals that were acquired by both systems. Three of these timing signals varied over the course of a single revolution, 1/rev, 256/rev, and an azimuthal ramp, and the fourth varied over the course of 20 revolutions, a step function that increased in level once per revolution.

3 Updated Transducer Labels

During the development of the HVAB blades, the labels used to identify the transducer locations were changed. This change applies only to the label for each transducer and not to the physical location of the transducer on the blade, these physical locations were consistent throughout the entire development process. The tables published in Overmeyer et al. [4] use the old labeling scheme. The data released with this file use the new labeling scheme, which is now considered the standard scheme and consistent with the engineering drawings for the blades. Tables 1 through 11 are updated versions of the tables, originally presented in Overmeyer et al., with the standard labeling scheme. In Tables 1 through 11, X, Y, and Z are the coordinates of the transducer in the global coordinate system as defined in Overmeyer et al. The global coordinate system (X,Y,Z), is defined relative to the center of rotation and is independent of blade twist/pitch. The +X direction is toward the tip, +Y direction is toward the leading edge and +Z direction is toward the upper surface. For a given blade station, a local coordinate system (η, ζ) is utilized and defined relative to the local airfoil quarter-chord point. The $+\eta$ direction is toward the trailing edge and $+\zeta$ is toward the upper surface.

The standard scheme numbers the transducers in numerical order by station, starting with Station 1, which is the station closest to the root of the blade. The first six transducers lie on the lower surface of the blade with the first transducer being closest to the the leading edge and the remaining five arranged in increasing distance from the leading edge. The pattern is then repeated on the upper surface with the seventh transducer being closest to the leading edge and the remaining 10 arranged in increasing distance from the leading edge. For example, the transducers on the lower surface of Station 1 are K001, K002, K003, K004, K005, and K006, with K001 being the lower surface transducer closest to the leading edge and K006 being the transducer closest to the trailing edge. The upper surface of Station 1 is populated with transducers K007 – K017, in numerical order with K007 being the closest to the leading edge and K017 being closest to the trailing edge. This arrangement can be seen in Table 1.

The only exception to this numbering scheme is Station 8. As seen in Table 8, the first three transducers are rearranged from the standard scheme. This exception was noted on the engineering drawings for the blades and was adopted here so that all the reference material for the blades would be consistent. This exception was also verified during the instrumentation checkout of the Hover blade prior to the beginning of testing. This numbering scheme for Station 8 is also consistent with the release of the blade pressure data, as discussed in Section 5.

4 Overview of the Data Reduction

The blade pressure data are presented by tip Mach number and collective. Data for each collective were acquired over multiple points and the average values and uncertainties are derived from the average value of the pressure for each of the points for that collective. For each point, data were acquired for 128 revolutions of the rotor and for the raw data, there were approximately 2500 samples/rev for Run 72 and 2300 samples/rev for Run 77. Run 72 was conducted at a nominal tip Mach number of 0.60 and data were collected for collective angles of 4.0°, 5.0°, 6.0°, 7.0°, 8.0°, 9.0°, 10.0°, 11.0°, and 12.0°. Run 77 was conducted at a nominal tip Mach number of 0.65 and data were collected for collective angles of 4.0°, 6.0°, 8.0°, 10.0°, 11.0°, 12.0°, and 13.0°. Data for each collective were comprised of a set of nominally 10 points. In Run 72, 3 of the

collective angles had 11 points and 1 had 13 points. For Run 77, 1 collective had 11 points, 2 had 9 points, and 1 had 7 points.

The pressure coefficients are normalized by the local dynamic pressure, which is based on the local speed at the station, $\Omega r_{nominal})_n$, where $r_{nominal})_n$ is the nominal radius for Station n. The pressure coefficient is then defined as:

$$C_P = \frac{(P - P_\infty)}{\frac{1}{2}\rho_\infty(\Omega r_{nominal})_n)^2}$$

where P_∞ is the average static pressure and ρ_∞ is the average density. These average values, along with the average value of the RPM, are provided in the data contained in the performance section the website.

5 Description of the Spreadsheet Data

For this first release of the blade pressure data, the spreadsheet is named `bladePressures_v1_2023_10.xlsx`. The spreadsheet contains two sheets, one for each of the tip Mach numbers that blade pressure data were acquired. The first sheet is named R72M600 for data from Run 72, which was conducted at a tip Mach number of 0.600, and the second sheet is named R77M650 for data from Run 77, which was conducted at a tip Mach number of 0.650. The layout on each sheet is identical. The first column contains the transducer label. The second column is the radial location of the transducer. The third column is the station number and the fourth column is the radial location of the station. The fifth column indicates the location of the transducer on the upper or lower surface of the blade. A value of zero (0) indicates that the transducer is on the lower surface and a value of one (1) indicates that the transducer is on the upper surface. The sixth column is the x/C location for that transducer.

For a given station, the upper line of transducers and the lower line of transducers are slightly staggered radially from one another in order to physically pack the transducers in the blade. This is the reason for a radial location for each transducer and a radial location for the station. The coordinates given in the spreadsheet are consistent with the description in Overmeyer et al. [4] and also in Tables 1 through 11 in this document. The coordinate, x/C, is defined similarly to the local coordinate, η/C, with the exception that the origin for x/C is at the leading edge as opposed to the quarter-chord point.

Following the sixth column in the sheet, is a set of four columns for each collective angle acquired during the run. Two columns for the mean absolute pressure value, P_{mean}, and its uncertainty, U_P. The units for both of these values are in psi, pounds-force/square-inch. These two values are taken together as, for example, $P_{K001} = P_{mean} \pm U_P \; psi$. The next two columns are for the coefficient of pressure based upon the local radial dynamic pressure and its uncertainty. The mean C_P value and its uncertainty, U_{C_P}, are taken together as for the pressure values, again for example, $C_P)_{K001} = C_P \pm U_{C_P}$. This grouping of four columns is repeated at each collective angle. The approach to quantifying the uncertainties is unchanged from that presented in Norman et al. [1].

The transducers damaged during the blade fabrication are indicated in the sheet by a value of zero (0) for all of the data in the corresponding cells for that transducer. The damage to these transducers is such that there is no data available for these transducers. Locations in the sheet where no data are provided, i.e., the cell is empty, are transducers that require further processing. It is possible that data for some of these locations will be available in future releases of the data.

Finally, some comments about K162 will be provided here. K162 is unique among the transducers in the fact that after blade fabrication; there was a large zero shift in the output of the transducer. The point at which the transducer stops responding to changes in pressure is now well within the pressure range of the data presented here. This is particularly true at high values of the collective. Above its minimum pressure, the output of K162 is linear but not to the same degree as the other transducers. The standard error of the regression for K162 is thus larger than the other transducers and this is reflected in its larger uncertainty range.

References

[1] Norman, T. R., Heineck, J. T., Schairer, E. T., Schaeffler, N. W., Wagner, L. N., Yamauchi, G. K., Overmeyer, A. D., Ramasamy, M., Cameron, C. G., Dominguez, M., and Sheikman, A. L., "Fundamental Test of a Hovering Rotor: Comprehensive Measurements for CFD Validation," VFS 79th Annual Forum Paper 1166, 2023.

[2] Wong, O. D., Noonan, K. W., Watkins, A. N., Jenkins, L. N., and Yao, C. S., "Non-Intrusive Measurements of a Four-Bladed Rotor in Hover - A First Look," Specialists Conference Paper, American Helicopter Society Aeromechanics Specialists Conference, San Francisco, CA, January 2010.

[3] Overmeyer, A. D. and Martin, P. B., "Measured Boundary Layer Transition and Rotor Hover Performance at Model Scale," AIAA Paper 2017-1872, AIAA SciTech 55th Aerospace Sciences Meeting, Grapevine, TX, 9-13 January 2017.

[4] Overmeyer, A. D., Copp, P. A., and Schaeffler, N. W., "Hover Validation and Acoustic Baseline Blade Set Definition," NASA TM-2020-5002153, May 2020.

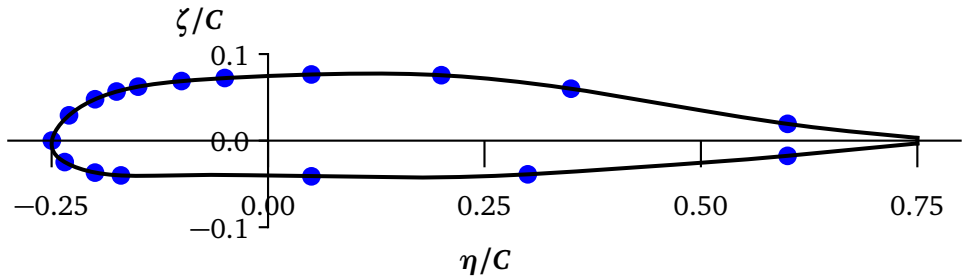

Figure 1: Station 1, Hover Blade - Kulite® Locations

Table 1: Station 1, Hover Blade - Nominal r/R: 0.397, Kulites® 1 – 17

Kulite®	X (in)	Y (in)	Z (in)	r/R	η/C	ζ/C
K001	25.890	1.287	-0.021	0.389	-0.235	-0.025
K002	25.890	1.103	-0.104	0.389	-0.200	-0.037
K003	25.890	0.942	-0.136	0.389	-0.170	-0.040
K004	25.890	-0.252	-0.248	0.389	0.050	-0.041
K005	25.890	-1.610	-0.356	0.389	0.300	-0.039
K006	25.890	-3.249	-0.385	0.389	0.600	-0.018
K007	26.910	1.356	0.116	0.405	-0.250	0.000
K008	26.910	1.235	0.265	0.405	-0.230	0.029
K009	26.910	1.063	0.352	0.405	-0.200	0.048
K010	26.910	0.924	0.389	0.405	-0.175	0.057
K011	26.910	0.786	0.408	0.405	-0.150	0.062
K012	26.910	0.511	0.420	0.405	-0.100	0.069
K013	26.910	0.238	0.416	0.405	-0.050	0.072
K014	26.910	-0.307	0.392	0.405	0.050	0.076
K015	26.910	-1.122	0.318	0.405	0.200	0.076
K016	26.910	-1.928	0.164	0.405	0.350	0.060
K017	26.910	-3.268	-0.172	0.405	0.600	0.019

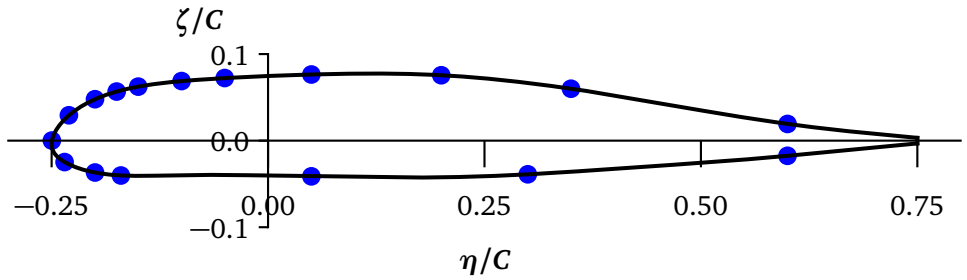

Figure 2: Station 2, Hover Blade - Kulite® Locations

Table 2: Station 2, Hover Blade - Nominal r/R: 0.598, Kulites® 18 – 34

Kulite®	X (in)	Y (in)	Z (in)	r/R	η/C	ζ/C
K018	39.600	1.285	-0.086	0.595	-0.235	-0.025
K019	39.600	1.096	-0.159	0.595	-0.200	-0.037
K020	39.600	0.934	-0.184	0.595	-0.170	-0.040
K021	39.600	-0.264	-0.235	0.595	0.050	-0.041
K022	39.600	-1.626	-0.274	0.595	0.300	-0.039
K023	39.600	-3.264	-0.220	0.595	0.600	-0.018
K024	39.900	1.360	0.051	0.600	-0.250	0.000
K025	39.900	1.247	0.206	0.600	-0.230	0.029
K026	39.900	1.079	0.301	0.600	-0.200	0.048
K027	39.900	0.941	0.344	0.600	-0.175	0.057
K028	39.900	0.804	0.370	0.600	-0.150	0.062
K029	39.900	0.530	0.395	0.600	-0.100	0.069
K030	39.900	0.258	0.404	0.600	-0.050	0.072
K031	39.900	-0.288	0.406	0.600	0.050	0.076
K032	39.900	-1.105	0.371	0.600	0.200	0.076
K033	39.900	-1.918	0.256	0.600	0.350	0.060
K034	39.900	-3.272	-0.016	0.600	0.600	0.019

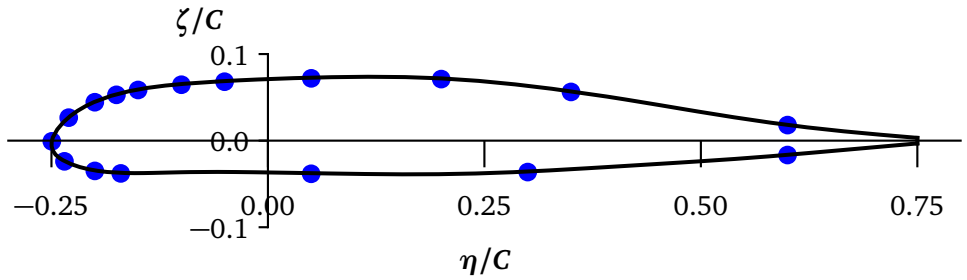

Figure 3: Station 3, Hover Blade - Kulite® Locations

Table 3: Station 3, Hover Blade - Nominal r/R: 0.673, Kulites® 35 – 51

Kulite®	X (in)	Y (in)	Z (in)	r/R	η/C	ζ/C
K035	44.588	1.283	-0.105	0.670	-0.235	-0.024
K036	44.588	1.093	-0.169	0.670	-0.200	-0.035
K037	44.588	0.930	-0.188	0.670	-0.170	-0.038
K038	44.588	-0.268	-0.214	0.670	0.050	-0.038
K039	44.588	-1.631	-0.230	0.670	0.300	-0.036
K040	44.588	-3.268	-0.155	0.670	0.600	-0.017
K041	44.888	1.360	0.021	0.675	-0.250	-0.001
K042	44.888	1.251	0.168	0.675	-0.230	0.027
K043	44.888	1.085	0.262	0.675	-0.200	0.044
K044	44.888	0.948	0.306	0.675	-0.175	0.053
K045	44.888	0.811	0.334	0.675	-0.150	0.059
K046	44.888	0.538	0.362	0.675	-0.100	0.065
K047	44.888	0.266	0.376	0.675	-0.050	0.068
K048	44.888	-0.280	0.387	0.675	0.050	0.072
K049	44.888	-1.098	0.367	0.675	0.200	0.071
K050	44.888	-1.913	0.271	0.675	0.350	0.056
K051	44.888	-3.272	0.037	0.675	0.600	0.018

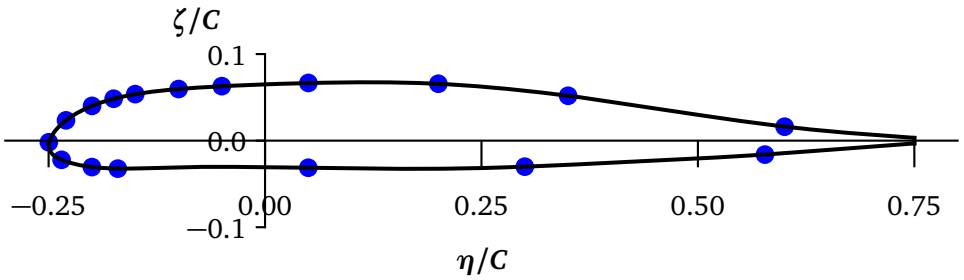

Figure 4: Station 4, Hover Blade - Kulite® Locations

Table 4: Station 4, Hover Blade - Nominal r/R: 0.748, Kulites® 52 – 68

Kulite®	X (in)	Y (in)	Z (in)	r/R	η/C	ζ/C
K052	49.575	1.281	-0.119	0.745	-0.235	-0.022
K053	49.575	1.090	-0.165	0.745	-0.200	-0.031
K054	49.575	0.927	-0.175	0.745	-0.170	-0.032
K055	49.575	-0.272	-0.171	0.745	0.050	-0.031
K056	49.575	-1.635	-0.166	0.745	0.300	-0.030
K057	49.575	-3.147	-0.092	0.745	0.577	-0.016
K058	49.875	1.361	-0.010	0.750	-0.250	-0.002
K059	49.875	1.253	0.128	0.750	-0.230	0.023
K060	49.875	1.089	0.219	0.750	-0.200	0.040
K061	49.875	0.953	0.264	0.750	-0.175	0.048
K062	49.875	0.817	0.293	0.750	-0.150	0.054
K063	49.875	0.544	0.325	0.750	-0.100	0.060
K064	49.875	0.272	0.343	0.750	-0.050	0.063
K065	49.875	-0.273	0.363	0.750	0.050	0.067
K066	49.875	-1.091	0.358	0.750	0.200	0.066
K067	49.875	-1.908	0.282	0.750	0.350	0.052
K068	49.875	-3.271	0.087	0.750	0.600	0.016

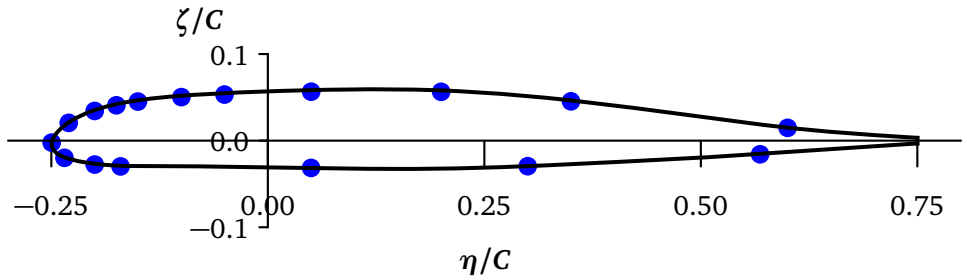

Figure 5: Station 5, Hover Blade - Kulite® Locations

Table 5: Station 5, Hover Blade - Nominal r/R: 0.823, Kulites® 69 – 85

Kulite®	X (in)	Y (in)	Z (in)	r/R	η/C	ζ/C
K069	54.563	1.278	-0.130	0.820	-0.235	-0.020
K070	54.563	1.087	-0.169	0.820	-0.200	-0.028
K071	54.563	0.924	-0.178	0.820	-0.170	-0.030
K072	54.563	-0.275	-0.167	0.820	0.050	-0.031
K073	54.563	-1.638	-0.133	0.820	0.300	-0.030
K074	54.563	-3.099	-0.033	0.820	0.568	-0.016
K075	54.863	1.360	-0.037	0.825	-0.250	-0.002
K076	54.863	1.255	0.089	0.825	-0.230	0.021
K077	54.863	1.093	0.167	0.825	-0.200	0.034
K078	54.863	0.957	0.205	0.825	-0.175	0.041
K079	54.863	0.822	0.231	0.825	-0.150	0.045
K080	54.863	0.549	0.264	0.825	-0.100	0.050
K081	54.863	0.278	0.285	0.825	-0.050	0.053
K082	54.863	-0.267	0.313	0.825	0.050	0.057
K083	54.863	-1.085	0.327	0.825	0.200	0.056
K084	54.863	-1.903	0.282	0.825	0.350	0.045
K085	54.863	-3.269	0.140	0.825	0.600	0.015

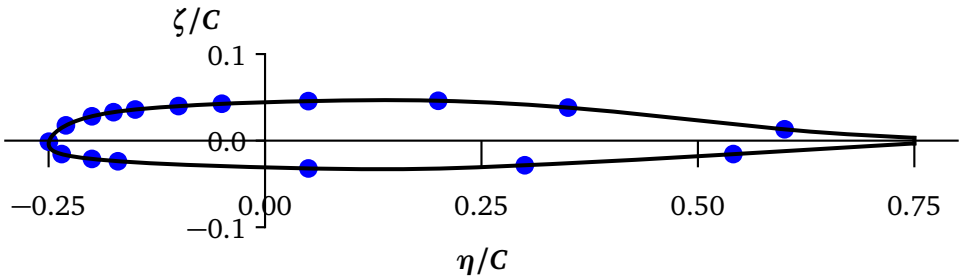

Figure 6: Station 6, Hover Blade - Kulite® Locations

Table 6: Station 6, Hover Blade - Nominal r/R: 0.873, Kulites® 86 – 102

Kulite®	X (in)	Y (in)	Z (in)	r/R	η/C	ζ/C
K086	57.888	1.277	-0.122	0.870	-0.235	-0.016
K087	57.888	1.086	-0.147	0.870	-0.200	-0.021
K088	57.888	0.922	-0.157	0.870	-0.170	-0.024
K089	57.888	-0.278	-0.167	0.870	0.050	-0.032
K090	57.888	-1.639	-0.107	0.870	0.300	-0.028
K091	57.888	-2.949	0.002	0.870	0.541	-0.016
K092	58.188	1.360	-0.048	0.875	-0.250	-0.001
K093	58.188	1.256	0.058	0.875	-0.230	0.018
K094	58.188	1.094	0.120	0.875	-0.200	0.028
K095	58.188	0.959	0.150	0.875	-0.175	0.033
K096	58.188	0.823	0.171	0.875	-0.150	0.036
K097	58.188	0.551	0.201	0.875	-0.100	0.040
K098	58.188	0.279	0.224	0.875	-0.050	0.043
K099	58.188	-0.265	0.257	0.875	0.050	0.046
K100	58.188	-1.082	0.284	0.875	0.200	0.046
K101	58.188	-1.900	0.266	0.875	0.350	0.038
K102	58.188	-3.267	0.171	0.875	0.600	0.013

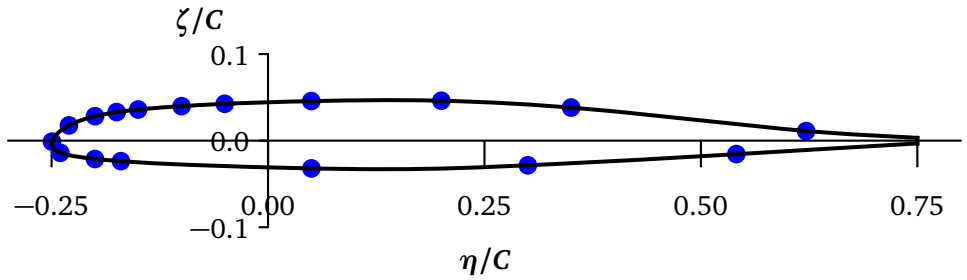

Figure 7: Station 7, Hover Blade - Kulite® Locations

Table 7: Station 7, Hover Blade - Nominal r/R: 0.898, Kulites® 103 – 119

Kulite®	X (in)	Y (in)	Z (in)	r/R	η/C	ζ/C
K103	59.550	1.304	-0.123	0.895	-0.240	-0.014
K104	59.550	1.085	-0.154	0.895	-0.200	-0.021
K105	59.550	0.921	-0.162	0.895	-0.170	-0.024
K106	59.550	-0.279	-0.165	0.895	0.050	-0.032
K107	59.550	-1.640	-0.097	0.895	0.300	-0.028
K108	59.550	-2.949	0.020	0.895	0.541	-0.016
K109	59.850	1.359	-0.056	0.900	-0.250	-0.001
K110	59.850	1.256	0.050	0.900	-0.230	0.018
K111	59.850	1.094	0.114	0.900	-0.200	0.028
K112	59.850	0.959	0.145	0.900	-0.175	0.033
K113	59.850	0.824	0.166	0.900	-0.150	0.036
K114	59.850	0.552	0.197	0.900	-0.100	0.040
K115	59.850	0.281	0.222	0.900	-0.050	0.043
K116	59.850	-0.263	0.259	0.900	0.050	0.046
K117	59.850	-1.081	0.291	0.900	0.200	0.046
K118	59.850	-1.899	0.278	0.900	0.350	0.038
K119	59.850	-3.383	0.184	0.900	0.622	0.011

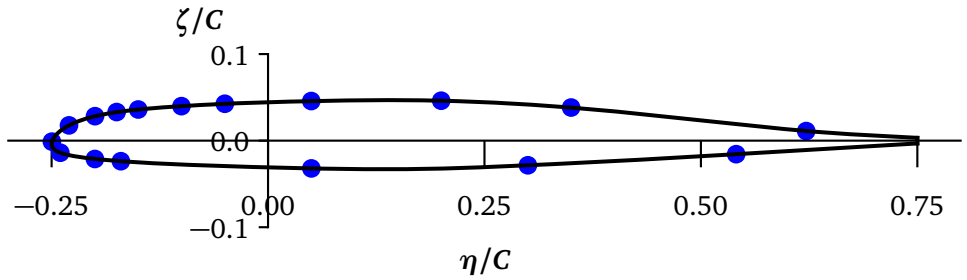

Figure 8: Station 8, Hover Blade - Kulite® Locations

Table 8: Station 8, Hover Blade - Nominal r/R: 0.928, Kulites® 120 – 136

Kulite®	X (in)	Y (in)	Z (in)	r/R	η/C	ζ/C
K121	61.545	1.303	-0.132	0.925	-0.240	-0.014
K122	61.545	1.084	-0.162	0.925	-0.200	-0.021
K120	61.545	0.920	-0.169	0.925	-0.170	-0.024
K123	61.545	-0.280	-0.163	0.925	0.050	-0.032
K124	61.545	-1.641	-0.085	0.925	0.300	-0.028
K125	61.545	-2.948	0.041	0.925	0.541	-0.016
K126	61.845	1.359	-0.066	0.930	-0.250	-0.001
K127	61.845	1.256	0.041	0.930	-0.230	0.018
K128	61.845	1.095	0.106	0.930	-0.200	0.028
K129	61.845	0.960	0.138	0.930	-0.175	0.033
K130	61.845	0.825	0.160	0.930	-0.150	0.036
K131	61.845	0.554	0.193	0.930	-0.100	0.040
K132	61.845	0.282	0.220	0.930	-0.050	0.043
K133	61.845	-0.261	0.261	0.930	0.050	0.046
K134	61.845	-1.078	0.299	0.930	0.200	0.046
K135	61.845	-1.897	0.292	0.930	0.350	0.038
K136	61.845	-3.382	0.209	0.930	0.622	0.011

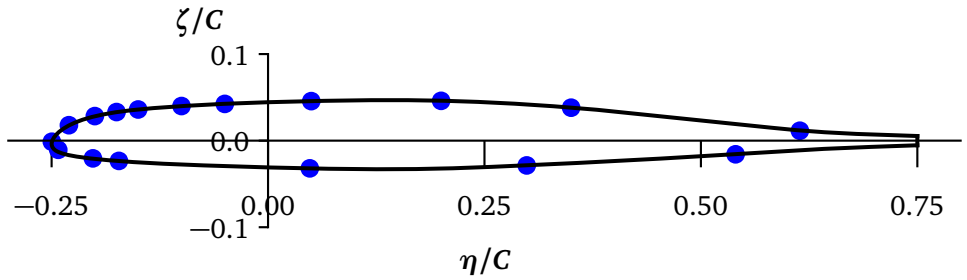

Figure 9: Station 9, Hover Blade - Kulite® Locations

Table 9: Station 9, Hover Blade - Nominal r/R: 0.953, Kulites® 137 – 153

Kulite®	X (in)	Y (in)	Z (in)	r/R	η/C	ζ/C
K137	63.208	1.303	-0.122	0.950	-0.242	-0.011
K138	63.208	1.083	-0.165	0.950	-0.202	-0.020
K139	63.208	0.919	-0.173	0.950	-0.172	-0.023
K140	63.208	-0.281	-0.161	0.950	0.048	-0.032
K141	63.208	-1.641	-0.076	0.950	0.299	-0.029
K142	63.208	-2.948	0.058	0.950	0.540	-0.016
K143	63.508	1.123	-0.072	0.955	-0.250	-0.001
K144	63.508	1.025	0.033	0.955	-0.230	0.018
K145	63.508	0.871	0.096	0.955	-0.200	0.028
K146	63.508	0.741	0.127	0.955	-0.175	0.033
K147	63.508	0.611	0.149	0.955	-0.150	0.036
K148	63.508	0.350	0.183	0.955	-0.100	0.040
K149	63.508	0.089	0.209	0.955	-0.050	0.042
K150	63.508	-0.433	0.252	0.955	0.050	0.046
K151	63.508	-1.218	0.293	0.955	0.200	0.046
K152	63.508	-2.006	0.291	0.955	0.350	0.038
K153	63.508	-3.396	0.221	0.955	0.614	0.011

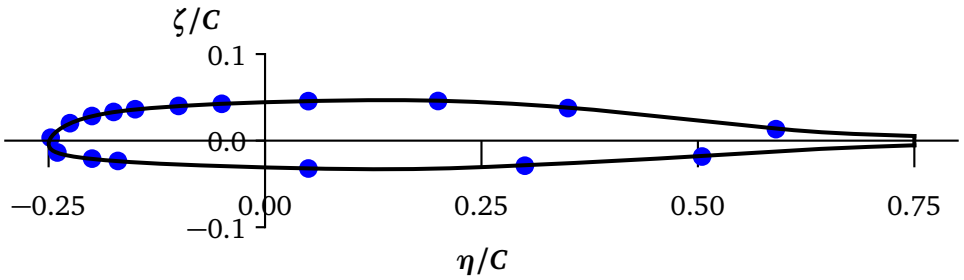

Figure 10: Station 10, Hover Blade - Kulite® Locations

Table 10: Station 10, Hover Blade - Nominal r/R: 0.971, Kulites® 154 – 170

Kulite®	X (in)	Y (in)	Z (in)	r/R	η/C	ζ/C
K154	64.405	0.409	-0.123	0.968	-0.240	-0.014
K155	64.405	0.221	-0.146	0.968	-0.200	-0.021
K156	64.405	0.082	-0.151	0.968	-0.170	-0.023
K157	64.405	-0.942	-0.137	0.968	0.050	-0.032
K158	64.405	-2.102	-0.060	0.968	0.300	-0.029
K159	64.405	-3.050	0.040	0.968	0.505	-0.018
K160	64.705	0.227	-0.045	0.973	-0.248	0.003
K161	64.705	0.132	0.035	0.973	-0.225	0.020
K162	64.705	0.021	0.078	0.973	-0.200	0.028
K163	64.705	-0.089	0.105	0.973	-0.175	0.033
K164	64.705	-0.199	0.125	0.973	-0.150	0.036
K165	64.705	-0.421	0.154	0.973	-0.100	0.040
K166	64.705	-0.642	0.177	0.973	-0.050	0.043
K167	64.705	-1.086	0.215	0.973	0.050	0.046
K168	64.705	-1.752	0.252	0.973	0.200	0.046
K169	64.705	-2.421	0.252	0.973	0.350	0.038
K170	64.705	-3.495	0.202	0.973	0.590	0.013

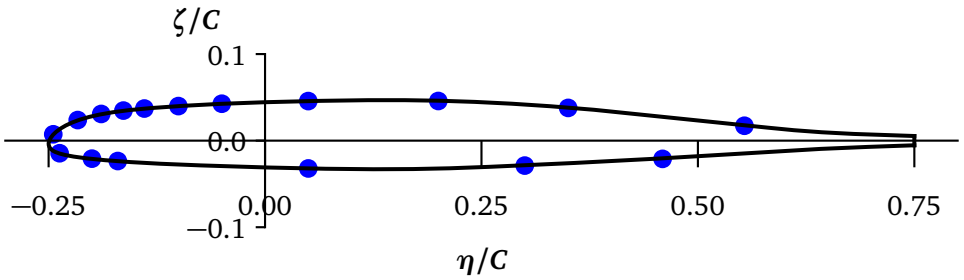

Figure 11: Station 11, Hover Blade - Kulite® Locations

Table 11: Station 11, Hover Blade - Nominal r/R: 0.988, Kulites® 171 – 187

Kulite®	X (in)	Y (in)	Z (in)	r/R	η/C	ζ/C
K171	65.535	-0.432	-0.110	0.985	-0.237	-0.015
K172	65.535	-0.579	-0.126	0.985	-0.200	-0.021
K173	65.535	-0.696	-0.130	0.985	-0.170	-0.024
K174	65.535	-1.556	-0.114	0.985	0.050	-0.032
K175	65.535	-2.530	-0.045	0.985	0.300	-0.029
K176	65.535	-3.149	0.021	0.985	0.459	-0.021
K177	65.835	-0.620	-0.026	0.990	-0.245	0.007
K178	65.835	-0.721	0.041	0.990	-0.216	0.024
K179	65.835	-0.820	0.073	0.990	-0.189	0.031
K180	65.835	-0.914	0.093	0.990	-0.164	0.035
K181	65.835	-1.003	0.107	0.990	-0.139	0.037
K182	65.835	-1.148	0.126	0.990	-0.100	0.040
K183	65.835	-1.333	0.147	0.990	-0.050	0.043
K184	65.835	-1.702	0.180	0.990	0.050	0.046
K185	65.835	-2.258	0.213	0.990	0.200	0.046
K186	65.835	-2.815	0.216	0.990	0.350	0.038
K187	65.835	-3.573	0.184	0.990	0.554	0.017